DOI: 10.1534/genetics.105.044842

Chromosome Complement of the Fungal Plant Pathogen *Fusarium graminearum* Based on Genetic and Physical Mapping and Cytological Observations

L. R. Gale,* J. D. Bryant,† S. Calvo,‡ H. Giese,§ T. Katan, K. O'Donnell,†† H. Suga,‡‡ M. Taga,§§ T. R. Usgaard,†† T. J. Ward†† and H. C. Kistler*,†,[1]**

**Cereal Disease Laboratory, U.S. Department of Agriculture, Agricultural Research Service, St. Paul, Minnesota 55108, †Department of Plant Pathology, University of Minnesota, St. Paul, Minnesota 55108, ‡ Broad Institute of MIT and Harvard University, Cambridge, Massachusetts 02141, §Department of Ecology, Section of Genetics and Microbiology, Royal Veterinary and Agricultural University, Copenhagen, DK-1871 Frederiksberg C Denmark, **Volcani Center, 50250 Bet Dagan, Israel, ††National Center for Agricultural Utilization Research, U.S. Department of Agriculture, Agricultural Research Service, Peoria, Illinois 61604, ‡‡Life Science Research Center, Division of Genomics Research, Gifu University, Gifu 501-1193, Japan and §§Department of Biology, Faculty of Science, Okayama University, Okayama 700-8530, Japan*

Manuscript received April 25, 2005
Accepted for publication July 28, 2005

ABSTRACT

A genetic map of the filamentous fungus *Fusarium graminearum* (teleomorph: *Gibberella zeae*) was constructed to both validate and augment the draft whole-genome sequence assembly of strain PH-1. A mapping population was created from a cross between mutants of the sequenced strain (PH-1, NRRL 31084, originally isolated from Michigan) and a field strain from Minnesota (00-676, NRRL 34097). A total of 111 ascospore progeny were analyzed for segregation at 235 loci. Genetic markers consisted of sequence-tagged sites, primarily detected as dCAPS or CAPS ($n = 131$) and VNTRs ($n = 31$), in addition to AFLPs ($n = 66$) and 7 other markers. While most markers exhibited Mendelian inheritance, segregation distortion was observed for 25 predominantly clustered markers. A linkage map was generated using the Kosambi mapping function, using a LOD threshold value of 3.5. Nine linkage groups were detected, covering 1234 cM and anchoring 99.83% of the draft sequence assembly. The nine linkage groups and the 22 anchored scaffolds from the sequence assembly could be assembled into four chromosomes, leaving only five smaller scaffolds (59,630 bp total) of the nuclear DNA unanchored. A chromosome number of four was confirmed by cytological karyotyping. Further analysis of the genetic map data identified variation in recombination rate in different genomic regions that often spanned several hundred kilobases.

FUSARIUM graminearum Schwabe, a haploid ascomycetous fungus and the major causal agent of Fusarium head blight (FHB) disease of small grain cereal crops, has received considerable attention by the scientific community due to severe disease outbreaks in the United States since 1992 (McMullen *et al.* 1997). These epidemics resulted in heavy yield losses, which were exacerbated by the fact that FHB-infected grain is often contaminated with trichothecene mycotoxins and estrogenic compounds that pose a serious threat to food and feed safety. Largely because outbreaks of the disease occurred only sporadically throughout the last century, the fungus and the disease were poorly studied before the 1990s. Since then, considerable resources (for example, through the U.S. Wheat and Barley Scab Initiative, www.scabusa.org) have been allocated to study the biology, toxicology, and epidemiology of the pathogen and to explore potential control measures, especially through plant varietal development and biotechnology.

Due to this national and international interest [the pathogen also causes serious problems in Canada, Asia, Europe, and parts of South America (McMullen *et al.* 1997)], *F. graminearum* was identified as a priority for whole-genome sequencing by the Broad Institute's Fungal Genome Initiative and in spring 2003 became the second plant-pathogenic fungus for which the whole-genome sequence has been made publicly available (http://www.broad.mit.edu). While a formal report detailing its genome structure is forthcoming, some generalizations can be made. Repetitive or even duplicated DNA is rare (Gale *et al.* 2002), and a preliminary report indicated that its karyotype consists of only four chromosomes (M. Taga, C. Waalwijk, W. G. Flier and G. H. J. Kema, unpublished results), a very low number compared to that in other filamentous fungi (*e.g.*, Zolan 1995). Perhaps due to these characteristics, the draft genome assembly of *F. graminearum* is remarkably complete, having fewer and larger scaffolds (supercontigs) than the assemblies of four other filamentous

Data for the whole-genome sequence of *F. graminearum* strain PH-1 have been deposited with the EMBL/GenBank Data Libraries under accession no. AACM01000000.

[1]*Corresponding author:* USDA, ARS, Cereal Disease Laboratory, University of Minnesota, 1551 Lindig St., St. Paul, MN 55108. E-mail: hckist@umn.edu

ascomycetous fungi (*Magnaporthe grisea*, *Neurospora crassa*, *Aspergillus nidulans*, and *Staganospora nodorum*) of comparable genome size (30–40 Mb) and sequencing coverage (7- to 13-fold). Despite the high quality of the *F. graminearum* draft sequence assembly, physical alignment of scaffolds into chromosomes has not been possible. The pulsed-field gel electrophoresis method that allows for separation and quantification of chromosomes for many fungi is not useful for *F. graminearum* because its chromosomes are comparatively large and similar in size.

In addition to the greatly expanded knowledge of the *F. graminearum* genome, significant advancement has been made regarding its evolutionary history and population genetic structure. Investigations of species limits based on genealogical concordance phylogenetic species recognition have determined that *F. graminearum* is not a single panmictic species, but a species complex [hereafter referred to as the *F. graminearum* (Fg) species complex] with at least nine phylogenetically and biogeographically distinct species that have been formally described (O'Donnell *et al.* 2000, 2004). The name *F. graminearum* was retained for the species previously designated as *F. graminearum*, lineage 7 (O'Donnell *et al.* 2000) and corresponds to the meiosporic state (teleomorph), *Gibberella zeae* (Schwein.) Petch (O'Donnell *et al.* 2004). To avoid confusion and to underscore its affiliation with related asexual fusaria such as *F. oxysporum*, we refer to the fungus as *F. graminearum* rather than as *G. zeae*. *F. graminearum* is cosmopolitan and the predominant causal agent of head blight of small-grain cereals in the United States and Europe (O'Donnell *et al.* 2000; Zeller *et al.* 2004).

Members of the Fg species complex reproduce sexually and, even though they are homothallic (selfing), outcrossing appears to be common because populations display low levels of gametic disequilibrium (*e.g.*, Gale *et al.* 2002; Zeller *et al.* 2004). Although interspecific hybrids between members of the Fg species complex can be generated in the laboratory (Bowden and Leslie 1999), interspecific hybridization in nature appears to be relatively low as evidenced by the reciprocal monophyly of the nine Fg clade species (O'Donnell *et al.* 2004). A genetic map of *F. graminearum* based on AFLP markers has been published (Jurgensen *et al.* 2002); however, the phylogenetic evidence strongly suggests that this map was based on an interspecific cross between *F. graminearum* and *F. asiaticum* (O'Donnell *et al.* 2004). *F. asiaticum*, previously known as *F. graminearum*, lineage 6, is predominantly found in Asia (O'Donnell *et al.* 2000; Gale *et al.* 2002; H. Suga, G. W. Karugia, T. Ward, L. R. Gale, K. Tomimura, T. Nakajima, K. Kageyama and M. Hyakumachi, unpublished observations), but has also been identified in very low numbers from samples originating from Brazil and the United States (D. Starkey, unpublished results). In this *F. graminearum* × *F. asiaticum* cross, segregation distortion was prevalent in five of the nine linkage groups, and recombination suppression was indicated by the fact that more than half of the progeny did not show any crossovers within four linkage groups (Jurgensen *et al.* 2002).

We generated a genetic map for *F. graminearum* based on an intraspecific cross between a derivative (nitrate-nonutilizing, hygromycin resistant) of the strain used for whole-genome sequencing (PH-1, NRRL 31084) and a nitrate-nonutilizing mutant of a field strain from Minnesota (00-676, NRRL 34097). The objectives were to: (1) anchor the draft sequence assembly with the genetic map using sequence-tagged site markers; (2) gain understanding of genome organization and variability; (3) compare our intraspecific *F. graminearum* cross with the interspecific cross of Jurgensen *et al.* (2002); (4) reveal relationships between physical and genetic distance and, by integrating information from cytological observations, attempt to identify other physical characteristics of the chromosomes; and (5) generate judiciously placed molecular markers for population genetic analysis.

MATERIALS AND METHODS

Cross for mapping: *F. graminearum* is homothallic and normally enters the sexual cycle by selfing. Strains used for crossing need to carry complementary genetic markers to differentiate perithecia derived by selfing or outcrossing. Nitrate-nonutilizing (nit) mutants were chosen because they are easy to generate and recognize. Before strains were paired for crosses, nit mutants were generated from parental strains and phenotyped as nit1 or nitM mutants depending on their growth on media containing different nitrogen sources. Mutants of *nit1* are defective in the structural gene for nitrate reductase and grow poorly on minimal medium containing nitrate as the sole nitrogen source; *nitM* mutants are defective in genes controlling the biosynthesis of a molybdenum-containing cofactor required for wild-type growth on minimal medium containing hypoxanthine as a sole source of reduced nitrogen (Klittich and Leslie 1988). The nitM phenotype is epistatic to the nit1 phenotype and is conferred by an unknown number of loci (Bowden and Leslie 1992). Standard procedures for generating and characterizing *nit* mutants were used (Correll *et al.* 1987) with minor modifications; Czapek-Dox agar (CDA) replaced minimal medium as the basal medium, and the chlorate medium (to generate nit mutants) contained reduced amounts of or no L-asparagine, compared with the one originally described (Correll *et al.* 1987).

One parental strain was derived from PH-1, the sequenced strain originally isolated from corn in Michigan. The derived strain, PH-1-hyg2-1, was defective in nitrogen reduction (nitM phenotype) and was hygromycin resistant. The hygromycin-resistant phenotype (hygR) was generated by the integration of the hygromycin B phosphotransferase (*hph*) gene of *Escherichia coli* at the *Fst*12 locus (J.-R. Xu, unpublished results) by previously described methods (Hou *et al.* 2002). The other parental strain was a nitrate reductase (*nit*1) mutant of 00-676 (00-676-2), a field isolate of *F. graminearum* isolated from diseased wheat from Norman County, Minnesota, collected in July 2000.

The mycelial plug crossing method was used as previously described (Klittich and Leslie 1988; Bowden and Leslie 1999; Jurgensen *et al.* 2002), except that cirrhi from individual perithecia were harvested in 0.5-ml microfuge tubes

containing 320 μl of sterile 2.5% Tween 60 solution and thereafter kept at 4°.

Parents and single ascospore progeny were grown on CDA and mycelial plugs of each strain were stored in 25% glycerol at −80°. DNA was obtained from mycelia grown in liquid medium as previously described (Gale *et al.* 2002) and their concentrations were adjusted to 10 ng/μl. The genetic map was developed using 112 ascospore progeny from a single perithecium of a cross between PH-1-hyg2-1 (hygR, nitM, *Nit1*) × 00-676-2 (hygS, NitM, *nit*1). Hereafter, these strains are generally referred to as PH-1 and 00-676.

Parental strains and the ascospore mapping population are available from the Fungal Genetics Stock Center (http://www.fgsc.net) as original parents PH-1-hyg2-1 (hygR, nitM, *Nit1*), FGSC 9602; 00-676-2 (hygS, NitM, *nit*1), FGSC 9603; and progeny (FGSC 9604–9685, A1–A82, nit1 or nitM and FGSC 9686–9715, WA1–WA30, recombinant prototrophic ascospore progeny).

Sequence-tagged site markers: As the genome sequence was not yet available at the beginning of the mapping project, initial primers for sequencing were designed on the basis of contigs generated from expressed sequence tags (ESTs) (Trail *et al.* 2002). Three cDNA libraries had been generated from carbon- and nitrogen-starved mycelia and from maturing perithecia of strain PH-1, resulting in 1088 contigs from 7996 ESTs. We designed primers for 318 contigs (>900 bp), using Web Primer (http://seq.yeastgenome.org/cgi-bin/web-primer) to amplify sequences that averaged 963 bp on the basis of cDNA. Amplifications were performed with AmpliTaq DNA Polymerase (Applied Biosystems, Foster City, CA), and amplification products were purified using Montage PCR Cleanup filter plates (Millipore, Billerica, MA). Sequencing reactions were performed using ABI BigDye version 3.0 sequencing chemistry (Applied Biosystems). Reaction products were purified via ethanol precipitation and run on an ABI3100 or ABI3730 genetic analyzer (Applied Biosystems). DNA sequences for PH-1 and 00-676 were edited and aligned using Sequencher version 4.1.2 (Gene Codes, Ann Arbor, MI) to identify polymorphisms. Parental polymorphisms were analyzed using GENETYX-Mac version 9.0 (Software Development, Tokyo) to determine whether differences in sequences [predominantly presenting themselves as single-nucleotide polymorphisms (SNPs)] coincided with a recognition site of a common restriction enzyme. If so, the cleaved amplified polymorphic sequence (CAPS) approach was used to visualize the two parental types in progeny DNA. If no diagnostic restriction site was present at the polymorphic site(s) that also could be assessed easily using agarose gel electrophoresis, derived CAPS (dCAPS) markers were developed using the web-based dCAPS Finder 2.0 (Neff *et al.* 2002). Mismatched primers of 29 or 30 bp length were identified that together with the parental polymorphism generated a unique restriction site in one of the parental sequences. The mismatched primer (one or two mismatches) was paired with a regular PCR primer (identified by Web Primer) ~200 bp 5′ or 3′ of the dCAPS primer. After digestion with the appropriate restriction enzyme, the two parental haplotypes were distinguished by agarose gel electrophoresis.

In addition to sequences based on ESTs, 13 partial DNA sequences of known genes were also generated to search for parental polymorphisms. Four genes were sequenced from the trichothecene toxin biosynthesis pathway (*TRI3*, *TRI4*, *TRI11*, and *TRI101*); the other genes were predominantly housekeeping genes and included translation elongation factor (*EF-1α*), β-tubulin, a predicted reductase (*RED*), the mating-type locus (genomic region spanning *MAT 1-1-2* and *MAT 1-1-3*), phosphate permease sections 1 and 2 (*PHO*), UTP-ammonia ligase sections 1 and 2 (*URA*), histone H3 (*H3*), a MAP kinase (*MGV1*), and a nonribosomal peptide synthetase (NRPS). Parts of the nuclear ribosomal intergenic spacer region (IGS) and a copy of the 5S rDNA, which is not part of the rDNA repeat but is dispersed 59 times in the genome of *F. graminearum* (Rooney and Ward 2005), were also sequenced. A number of these genes have been used previously to generate gene genealogies for the *F. graminearum* species complex (O'Donnell *et al.* 2000, 2004; Ward *et al.* 2002). Parts of two additional genes (*Tri*5, ITS) were not sequenced, but PCR products were examined on agarose gels for potential parental polymorphisms in restriction sites using nine common restriction enzymes.

The whole-genome sequence of strain PH-1 became available after most of the primers for the loci listed above had been designed and sequenced for both parents. Subsequently, all loci (with one exception, HK235) could be aligned with the whole-genome sequence. With only one exception, all polymorphic markers were located on the nine largest scaffolds that range in size from 734,521 to 8,822,436 bp. Ensuing efforts for marker identification in parental strains concentrated on identifying polymorphisms first in the smaller scaffolds, then in ends of larger scaffolds, and then, after preliminary linkage analysis, in gaps between initial linkage groups. Noncoding regions were targeted predominantly, as these sequences were expected to harbor a higher degree of polymorphism.

Variable number of tandem repeats (VNTR) markers were developed after the whole-genome sequence was released (Suga *et al.* 2004). VNTRs with repeat units of 2–18 nucleotides for the seven largest scaffolds were identified using Tandem Repeats Finder (Benson 1999) and primers were designed up- and downstream from 54 VNTR sites to amplify ~250 bp for each site (Suga *et al.* 2004). In addition to the VNTR markers developed by Suga *et al.* (2004) we screened an additional 47 VNTR loci located in genomic locations poorly represented by other markers favoring period sizes >5.

All oligonucleotide primers developed for this project are labeled HK*xx*, with *xx* denoting numbers for the forward primer of a particular primer pair; the reverse primer was assigned the number subsequent to the forward primer number.

All sequence-based markers were organized into a FASTA-formatted file and subjected to batch BLAST analysis against the sequence assembly of *F. graminearum* to generate sequence-tagged sites (STSs). Genomic locations (scaffold, contig number, and position of the amplified fragment within contig) were determined for each STS. The exact physical location of the assessed polymorphic site was computed for markers assessed by SNPs, while for VNTR markers, fragment length polymorphisms (FLPs), and plus/minus markers, the midpoint of the amplified fragment within contigs was determined.

PCR was carried out either in a PTC-100 Peltier thermal cycler (MJ Research, Waltham, MA) or in a Robocycler Gradient 96 temperature cycler (Stratagene, La Jolla, CA) as follows: total volume of the reaction mixture was 10 μl containing 10 mm Tris-HCl pH 8.3, 50 mm KCl, 1.5 mm $MgCl_2$, 200 μm of each dNTP, 1 μm of each primer, 0.25 unit *Taq* polymerase (Takara Mirus Bio, Madison, WI), and 10 ng genomic DNA. Cycling conditions were: 95° for 2 min; then 30 cycles of 95° for 1 min, 58° for 1 min, 72° for 1 min; and a final extension at 72° for 10 min. In a few instances the annealing temperature was reduced to 52° or 47°. CAPS products were usually resolved in 1.5% agarose gels (SeaKem LE agarose; Cambrex Bio Science, Rockland, ME), while products from dCAPS and VNTR markers were separated in 3% MetaPhor agarose gels (Cambrex Bio Science), containing 0.5 μg/ml ethidium bromide in gels, followed by visualization over a UV transilluminator.

A number of loci that were to be analyzed by dCAPS were poorly amplified with the mismatched dCAPS primers. In those instances, amplification was first performed using the original primers for that locus, amplifying ~1 kb of sequence; 2 μl of the resulting PCR product was treated with 0.8 unit shrimp alkaline phosphatase and 4 units Exonuclease I (Exo I) to degrade the initial set of primers. The reaction was incubated at 37° for 15 min and deactivated at 80° for 15 min in a thermal cycler. Thereafter, 97 μl H_2O was added to each tube and PCR reactions were set up using the dCAPS primers and performed as described above, except that genomic DNA was replaced with 1 μl of this new template. Amplification products were generally much improved after this procedure.

AFLP markers: AFLP markers were generated and analyzed as described in Vos *et al.* (1995) and Justesen *et al.* (2002). For preamplification P- and M-primers were used, corresponding to their respective adapters. For selective amplification, two selective nucleotides were added to each primer. For the *Pst*I primer either AA or AC was used while 12 different combinations of selective nucleotides were used for the *Mse*I primers. Fourteen primer combinations were used in the final mapping procedure. AFLP markers were named according to primer combination and size of PCR fragment (*e.g.*, PACMTG-750).

Data analyses: While AFLP markers were scored as present or absent, STS markers (predominantly assessed as CAPS, dCAPS, and VNTR) were generally scored by differences in fragment sizes, with or without prior restriction with common enzymes. One ascospore progeny (A15) showed both parental patterns with a number of markers and was presumed to be a mixed culture. Data for this progeny were discarded, leaving data from 111 progeny for final analyses. Assembly of the genetic map was done using JoinMap 3.0 (Van Ooijen and Voorrips 2001) via remote access to the Supercomputing Institute, University of Minnesota. In JoinMap, the mapping population was defined as a HAP population type, *i.e.*, a haploid population originating from one heterozygous individual with unknown linkage phases. JoinMap uses a weighted least-squares procedure that adds markers sequentially to the map (Stam 1993). A χ^2-test with $P < 0.05$ was used to test for expected segregation ratios of 1:1.

Generation of a framework map considered STS markers. The hyg and nit phenotypes were also included in initial analyses, as well as HK235, the only EST-based marker that could not be found in the sequence assembly. Assignment to linkage group was based on the logarithm of odds (LOD) threshold value, set initially at the default values of 2.0–10.0 using the Kosambi mapping function for calculation of pairwise distances. The resulting linkage order was then compared to their physical location in the sequence assembly. AFLP markers were added subsequently. Markers that did not map, that altered the physical position of other markers, or that had high χ^2-values were removed and the data were reanalyzed.

Data for the remaining markers were arranged sequentially for all progeny in a haplotype map that was color coded to indicate parental type. If there was a disagreement between physical position and their placement in the genetic map, STS markers were placed in the haplotype map according to their physical position. All putative single-locus double crossovers for STS markers were reevaluated to eliminate the possibility of mistyping. Non-STS (*i.e.*, AFLP) markers that were accepted into the map only after the final third round in the mapping procedure (no constraints of maximum allowed reduction in goodness-of-fit) were visually evaluated for their fit at the mapped location. If too many single-locus double crossovers were discerned for a number of progeny for placement of that marker, especially for genomic regions with little recombination, a subjective decision was made in favor of their removal.

Assigning linkage groups and scaffolds to chromosomes: For generation of the chromosome complement, we took advantage of the 43 scaffolds generated by the whole-genome sequence assembly and also included consideration of an improved assembly (T. J. Ward and K. O'Donnell, unpublished results) that established overlaps between scaffolds from the *F. graminearum* genome assembly that were not recognized by the assembly program ARACHNE (Batzoglou *et al.* 2002) but were identified on the basis of a combination of BLAST and manual sequence assembly analyses (Sequencher 4.1.2; Gene Codes, Ann Arbor, MI). On the basis of regions of perfect DNA sequence overlap, the 43 scaffolds generated by ARACHNE were manually reduced to 29 scaffolds. Overlaps between scaffolds were on average 658 bp (range: 423–932 bp). The smallest scaffold, scaffold 43 (contig 1.511 with 3070 bp), was determined to be contained entirely within another contig (base pairs 148,879–151,949 within contig 1.467). Among the 29 scaffolds, 2 belong to the mitochondrial genome (scaffolds 23 and 42) (J. Kennell, personal communication). Therefore, 27 scaffolds remained that needed to be integrated into the nuclear component of the genome. Scaffolds were aligned with linkage groups generated by genetic mapping and the chromosome complement was established by assembling the two interconnected data sets.

Cytology: Cytological observation of mitotic chromosomes was carried out by the germ tube burst method (GTBM) (Shirane *et al.* 1988; Taga and Murata 1994) followed by visualization via fluorescence microscopy. Macroconidia were produced in 40 ml mung bean broth in a 100-ml Erlenmeyer flask inoculated separately with both parental strains followed by shaking on a rotary shaker for 3–4 days at 20°–25°. Broth was prepared by boiling 40 g of mung beans in 1 liter of water for 10 min, after which it was filtered through cheesecloth before autoclaving. The conidial culture was filtered through one layer of Kimwipe to remove mycelia, and the conidia were washed twice with water by centrifugation. Finally, conidia were suspended in potato dextrose broth at a concentration of $\sim 4 \times 10^5$/ml. To prepare germlings that adhered to a slide, a droplet of conidial suspension (150–200 μl) was placed in a square (24 × 32 mm) lined with paper cement on a clean slide and incubated under humid conditions at 25° for 6–6.5 hr to allow germination. Slides were dipped in a staining jar containing water for ~30 sec to wash off the broth and excessive water on the slide was removed with filter paper. Slides were then immersed in a methanol:acetic acid solution [17:3; 99.5% methanol:glacial acetic acid (v/v)] for at least 20 min at room temperature to burst germ tubes and to fix samples chemically. After fixation, the slides were flame dried and stored at room temperature until use.

Chromosome specimens were mounted in fluorescence antifade solution (Johnson and Araujo 1981) containing 1 μg/ml DAPI, sealed with nail polish, and observed under an epifluorescence microscope (Nikon E600 equipped with UV-1A filter block) with a ×100 oil-immersion objective (N.A. 1.3). Photographs were taken on 35-mm ISO 400 reversal film (Fujichrome Provia 400F). Images were imported onto a personal computer with a film scanner (Nikon Coolscan IV) and processed with Adobe Photoshop 7.0. The length of the longitudinal axis of each chromosome was measured with Scion Image version 4.02 (Scion Corporation, Frederick, MD), using processed digital images.

Relationship between physical and genetic distance: After final map analyses, the physical distance between the polymorphisms of neighboring STS markers was calculated, taking into account the manually improved assembly and adjusting for the small duplicated sequences generated by overlaps. For the smaller scaffolds that mapped between larger scaffolds, we estimated their locations between contigs for distance

calculations. As we assumed a zero distance between scaffolds within chromosomes, the physical distance between markers located on different scaffolds was underestimated by an unknown distance. The genetic distance between two STS markers was also calculated, taking into account map contributions by AFLPs at the ends of linkage groups. Genetic distances between linkage groups within chromosomes were assumed to be 30 cM, perhaps underestimating actual (unknown) genetic distances. The relationship between recombination rate and physical distance along each chromosome for all STS markers was calculated by dividing total physical distance (in base pairs) by total map distance (in centimorgans) for each chromosome. This resulted in the average length of DNA at which a recombination rate of 1 cM was observed. All genetic map distances between STS markers were then converted to reflect the recombination rate between them if the physical distance between markers was assumed to be average.

RESULTS

Cross: The cross between PH-1-hyg2-1 (hygR, nitM, *Nit1*) and 00-676-2 (hygS, NitM, *nit*1) used for constructing the genetic map included as a parent a derivative of the strain used for shotgun whole-genome sequencing (PH-1). χ^2-analysis showed that the observed segregation of the nit phenotypes in the progeny [61 nitM, *Nit1* or nitM, *nit1*:21 NitM, *nit*1:30 wild-type (WT) NitM, *Nit1* recombinants] was not significantly different from the expected ratios of 2:1:1 ($P = 0.310$). However, the segregation ratio for resistance to hygromycin in the progeny was significantly different from the 1:1 expected ($P = 0.008$) due to an excess of sensitive (hygS) progeny.

STS markers: From 318 primer pairs that were designed on the basis of EST contigs, 303 sequences were generated for both parents, resulting in ~290 kb of sequence data for each parent. Of these sequences, 109 (36%) showed at least one polymorphic site between the parents. The 15 previously characterized loci that were sequenced covered another 17 kb per parent that contributed 6 polymorphic sequences for *EF-1*α, *MAT*, *RED*, β-tubulin, *TRI*4, and NRPS; the IGS and 5S rDNAs were polymorphic as well. *Tri*5 and the ribosomal ITS displayed no polymorphisms between the parents after restriction with nine enzymes. Using the draft sequence assembly of *F. graminearum* and sequencing target sites on smaller scaffolds, on ends of larger scaffolds, and on gaps between linkage groups generated by preliminary map analysis, another 34 polymorphic sites were identified.

Of a total of 151 polymorphic sites identified by the methods described above, progeny data for 11 loci were not collected due to their close physical proximity to other polymorphic loci in regions of low recombination. In addition, 3 loci could not be amplified after multiple trials and targeting a variety of putative primer sites. Two EST-based markers coincided with VNTR markers and were eventually scored as VNTR markers. Of the remaining 135 markers, 47 were analyzed as CAPS, 86 as dCAPS, and 2 as FLPs. Four genomic sites, all located on small scaffolds, seemingly were not present in 00-676 (no PCR amplification); of these, two present/absent (plus/minus) markers were used to generate progeny data.

Among the 54 VNTRs screened initially (Suga *et al.* 2004), 32 displayed size polymorphisms between the parents; data were collected for 27 loci. A subsequent screen of 47 VNTR loci, targeting previously unmapped regions of the sequence assembly, yielded six additional markers.

Resistance/sensitivity to hygromycin assessed as a phenotypic marker could also be sequence tagged, as the *hph* gene conferring resistance to hygromycin replaced *Fst*12, a gene with a known genomic location. The total number of polymorphic sequence-tagged loci that were included in initial map analysis was 169. One EST-based marker (HK235) did not match the genome sequence and therefore could not be aligned. However, sequences identical to HK235 were found in the "excluded reads" file of unassembled sequences from the Broad Institute sequencing project of *F. graminearum*. In addition, a BLASTN search revealed high sequence similarity between HK235 and a number of 28S ribosomal RNA genes and intergenic spacer sequences of other Fusarium species. We therefore conclude that HK235 belongs to the rDNA repeat that is not part of the sequence assembly currently available for *F. graminearum*.

AFLP markers: Twenty-four primer combinations were used to screen the parental isolates and the 14 most informative were selected for progeny analyses. Data were collected for 80 polymorphic marker bands, ranging in size from 90 to 750 bp. The number of polymorphic markers per primer combination ranged from 3 to 10 with an average of 5.6. Of the 80 bands, 43 were scored as present for PH-1 and 37 as present for 00-676. All 80 AFLP markers were included in preliminary map analyses.

Preliminary map analyses: A total of 111 progeny were analyzed initially for the 169 STSs, HK235, and the *nit* phenotypic marker. Thirteen linkage groups were obtained at LOD 3.5; among these, 6 contained four or fewer markers, including three unlinked markers that were placed in individual "linkage groups" (Table 1). The resulting preliminary map was compared to and aligned with the sequence-based physical map. Correspondence between physical location and genetic map position was colinear for nearly all markers, with the following exceptions: One STS marker, HK1273 (scaffold 3), was slightly out of order (~5 map units); *i.e.*, its placement in the genetic map was not colinear with its physical position. Genetic placement of HK663, a marker that defines the mating-type locus, also was questionable. This locus is located 231 kb away from the end of scaffold 5. Three smaller scaffolds genetically mapped with markers on scaffold 5 ahead of HK663 and away from markers in the succeeding scaffold 2 (Table 1). As it seems likely that the three smaller scaffolds are positioned between scaffold 5 and scaffold 2, rather

TABLE 1

Chromosome maps of *Fusarium graminearum*

Locus	Marker	Scaffold	Contig	PH-1[a]	00-676[b]	Missing data	χ^2	LG	Kos 3.5	LG	Kos 3.5	Hald 3.5
					Chromosome 1							
PACMGG-115	AFLP			57	54	0	0.1			IA	0.00	0.00
HK1123	CAPS	11	1.475	58	53	0	0.2	10	0.00	IA	6.10	6.50
HK1129	dCAPS	22	1.487	58	53	0	0.2	10	0.00	IA	6.10	6.50
PACMGG-420	AFLP			59	52	0	0.4			IA	26.19	31.65
PACMGT-360	AFLP			50	60	1	0.9			IA	47.29	59.83
PAAMCA-280	AFLP			46	63	2	2.6			IA	53.60	67.44
HK1237	dCAPS	1	1.5	47	64	0	2.6	1	0.00	IA	61.58	77.59
PAAMGG-250	AFLP			48	63	0	2			IA	65.81	82.80
PACMGC-350	AFLP			50	61	0	1.1			IA	69.84	87.83
HK929	dCAPS	1	1.6	50	61	0	1.1	1	10.96	IA	73.00	91.88
HK1041	VNTR	1	1.10	53	58	0	0.2	1	21.49	IA	83.68	105.14
PACMTG-355	AFLP	1	1.10	52	59	0	0.4			IA	84.90	106.49
HK1271	dCAPS	1	1.10	51	60	0	0.7	1	23.31	IA	85.61	107.23
HK881	CAPS	1	1.11	51	60	0	0.7	1	23.31	IA	85.61	107.23
HK627	dCAPS	1	1.11	51	60	0	0.7	1	23.31	IA	85.61	107.23
HK907	VNTR	1	1.12	51	60	0	0.7	1	23.31	IA	85.61	107.23
HK1025b	dCAPS	1	1.16	51	60	0	0.7	1	23.31	IA	85.61	107.23
HK1027	dCAPS	1	1.18	51	60	0	0.7	1	23.31	IA	85.61	107.23
HK1101	dCAPS	1	1.19	51	60	0	0.7	1	23.31	IA	85.61	107.23
HK1029	dCAPS	1	1.22	52	59	0	0.4	1	24.15	IA	86.46	108.13
HK677	dCAPS	1	1.34	52	59	0	0.4	1	27.48	IA	89.75	111.80
HK1107	dCAPS	1	1.35	54	57	0	0.1	1	33.05	IA	95.27	118.52
HK1031	dCAPS	1	1.37	55	56	0	0	1	36.07	IA	98.12	122.08
HK623	dCAPS	1	1.48	51	60	0	0.7	1	38.91	IA	100.89	125.40
HK1043	VNTR	1	1.52	51	60	0	0.7	1	38.91	IA	100.89	125.40
HK233	dCAPS	1	1.53	50	61	0	1.1	1	40.98	IA	102.88	127.74
HK231	dCAPS	1	1.56	51	60	0	0.7	1	44.52	IA	106.32	131.91
HK1045(=HK813)	VNTR	1	1.70	51	60	0	0.7	1	47.79	IA	109.54	135.73
HK1047	VNTR	1	1.72	51	60	0	0.7	1	47.79	IA	109.54	135.73
HK1231	dCAPS	1	1.77	51	60	0	0.7	1	47.79	IA	109.54	135.73
PAAMCA-375	AFLP			58	51	2	0.5			IA	118.94	147.17
HK931	dCAPS	1	1.89	56	55	0	0	1	60.65	IA	123.74	153.54
HK957	VNTR	1	1.91	57	54	0	0.1	1	66.82	IA	129.84	161.02
HK689	CAPS	1	1.91	59	52	0	0.4	1	69.88	IA	132.86	164.48
HK1205	dCAPS	1	1.92	65	46	0	3.3	1	89.28	IA	152.20	191.34
HK1261	CAPS	1	1.93	64	47	0	2.6	1	108.03	IA	170.94	215.60
HK1277	CAPS	1	1.93	66	45	0	4*	1	111.53	IA	174.44	219.33
HK1293	VNTR	1	1.94	74	37	0	12.3***	1	143.04	IA	205.94	262.50
HK1275	dCAPS	1	1.98	72	39	0	9.8**	1	144.89	IA	207.80	264.57
HK1229	dCAPS	1	1.100	71	40	0	8.7**	1	147.66	IA	210.59	267.67
HK919	VNTR	1	1.101	70	41	0	7.6**	1	148.58	IA	211.52	268.69
HK607	CAPS	1	1.103	70	41	0	7.6**	1	148.58	IA	211.52	268.69
HK625	dCAPS	1	1.110	69	42	0	6.6*	1	151.28	IA	214.18	271.67
HK1227	dCAPS	1	1.111	65	46	0	3.3	1	159.61	IA	222.12	281.05
HK667	dCAPS	1	1.111	65	46	0	3.3	1	160.89	IA	223.47	282.51
HK1035	dCAPS	1	1.111	65	46	0	3.3	1	160.89	IA	223.47	282.51
PACMTG-490	AFLP			62	49	0	1.5			IA	224.90	283.94
HK693	CAPS	1	1.111	63	48	0	2	1	166.25	IA	229.43	289.33
PACMTT-145	AFLP			63	48	0	2			IA	238.51	300.62
HK933	dCAPS	1	1.113	63	48	0	2	1	175.98	IA	239.69	301.90
HK959	VNTR	1	1.114	68	43	0	5.6*	1	188.69	IA	252.38	317.56
HK1111	dCAPS	1	1.114	65	46	0	3.3	1	193.04	IA	256.75	322.62
HK457b	CAPS	1	1.116	68	43	0	5.6*	1	212.58	IA	276.39	348.30
HK1225	dCAPS	1	1.116	67	44	0	4.8*	1	223.46	IA	287.25	361.28
HK1093	dCAPS	1	1.116	66	45	0	4*	1	227.69	IA	291.48	365.83
HK145(=HK449)	CAPS	1	1.116	67	44	0	4.8*	1	228.60	IA	292.40	366.81

(*continued*)

TABLE 1

(Continued)

Locus	Marker	Scaffold	Contig	PH-1[a]	00-676[b]	Missing data	χ^2	LG	Kos 3.5	LG	Kos 3.5	Hald 3.5
HK961	VNTR	1	1.122	60	51	0	0.7	1	258.72	IA	322.51	411.55
HK885	dCAPS	1	1.122	59	52	0	0.4	1	264.28	IA	328.08	418.14
HK941	dCAPS	7	1.412	52	59	0	0.4	1	272.59	IA	336.38	427.78
HK1001	VNTR	7	1.417	54	57	0	0.1	1	274.11	IA	337.91	429.37
HK209	CAPS	7	1.417	54	57	0	0.1	1	274.11	IA	337.91	429.37
HK1099	dCAPS	7	1.417	53	58	0	0.2	1	275.02	IA	338.81	430.34
HK431	CAPS	7	1.420	54	57	0	0.1	1	275.93	IA	339.72	431.32
HK863	CAPS	7	1.425	57	54	0	0.1	1	278.66	IA	342.45	434.31
HK1003	VNTR	7	1.437	50	61	0	1.1	1	288.17	IA	351.97	445.68
HK647	dCAPS	7	1.441	47	64	0	2.6	1	297.86	IA	361.66	457.59
PACMTb-305	AFLP			60	51	0	0.7			IB	0.00	0.00
PACMGT-290	AFLP			59	51	1	0.6			IB	0.63	0.63
HK1147	CAPS	7	1.446	56	55	0	0	2	0.00	IB	5.11	5.41
PACMCC-225	AFLP			54	55	2	0			IB	8.43	8.97
					Chromosome 2							
HK1185	Plus/minus	25	1.491	55	56	0	0	11	0.00	IIA	0.00	0.00
HK1289	dCAPS	5	1.323	56	54	1	0	11	13.99	IIA	12.99	15.16
PAAMAA-150	AFLP			51	53	7	0			IIA	21.20	24.30
PACMGG-320	AFLP			61	50	0	1.1			IIB	0.00	0.00
PAAMGA-590	AFLP			43	50	18	0.5			IIB	9.20	11.20
PAAMAA-120	AFLP			60	50	1	0.9			IIB	20.77	26.14
HK1303	VNTR	5	1.329	59	52	0	0.4	3	0.00	IIB	21.29	26.71
PAAMGA-255	AFLP			60	50	1	0.9			IIB	21.95	27.49
PACMCC-305	AFLP			59	50	2	0.7			IIB	34.19	43.96
PACMTb-640	AFLP			58	52	1	0.3			IIB	41.09	52.61
HK1219	dCAPS	5	1.335	57	54	0	0.1	3	21.68	IIB	43.20	54.89
HK245	CAPS	5	1.335	58	53	0	0.2	3	22.60	IIB	44.02	55.79
HK261	CAPS	5	1.338	59	52	0	0.4	3	23.51	IIB	44.83	56.68
HK229	dCAPS	5	1.338	59	52	0	0.4	3	23.51	IIB	44.83	56.68
HK951	dCAPS	5	1.340	58	53	0	0.2	3	23.90	IIB	45.26	57.09
HK1069	VNTR	5	1.341	58	53	0	0.2	3	23.90	IIB	45.26	57.09
HK1109	dCAPS	5	1.343	59	52	0	0.4	3	24.77	IIB	46.13	58.03
HK1005	dCAPS	5	1.349	59	52	0	0.4	3	24.77	IIB	46.13	58.03
HK785	CAPS	5	1.349	59	52	0	0.4	3	24.77	IIB	46.13	58.03
HK639	dCAPS	5	1.349	60	51	0	0.7	3	26.91	IIB	48.08	60.19
HK1203b	CAPS	5	1.350	60	51	0	0.7	3	26.91	IIB	48.08	60.19
HK645	dCAPS	5	1.354	60	51	0	0.7	3	31.72	IIB	52.90	65.79
HK995	VNTR	5	1.355	58	53	0	0.2	3	34.84	IIB	55.92	69.54
EF/HK879	dCAPS	5	1.355	58	53	0	0.2	3	37.00	IIB	57.97	71.97
HK997	VNTR	5	1.358	55	56	0	0	3	40.92	IIB	61.84	76.66
MAT/HK663	dCAPS	5	1.358	54	57	0	0.1	3	*44.48*	IIB	*65.31*	*80.52*
HK1139	CAPS	36	1.503	55	56	0	0	3	43.69	IIB	64.51	79.63
HK1177	CAPS	14	1.478	55	56	0	0	3	43.69	IIB	64.51	79.63
HK1207	dCAPS	13	1.477	55	56	0	0	3	43.69	IIB	64.51	79.63
HK1125	CAPS	13	1.477	55	56	0	0	3	43.69	IIB	64.51	79.63
HK621	dCAPS	2	1.141	55	56	0	0	3	43.69	IIB	64.51	79.63
HK1049	VNTR	2	1.142	51	60	0	0.7	3	54.48	IIB	75.15	92.30
PAAMAA-190	AFLP			51	56	4	0.2			IIB	85.88	105.94
HK203	dCAPS	2	1.145	54	57	0	0.1	3	74.89	IIB	94.23	120.47
PAAMTT-140	AFLP			55	52	4	0.1			IIB	102.19	129.81
HK193	CAPS	2	1.146	59	52	0	0.4	3	95.60	IIB	112.62	142.52
PACMGC-220	AFLP			59	52	0	0.4			IIB	119.84	150.96
HK1155	CAPS	2	1.147	64	47	0	2.6	3	108.79	IIB	126.25	158.25
PACMTT-395	AFLP			70	41	0	7.6**			IIB	138.93	175.43
HK1051	VNTR	2	1.148	62	49	0	1.5	3	130.00	IIB	147.64	185.33
RED	CAPS	2	1.150	51	60	0	0.7	3	156.63	IIB	156.57	206.97

(*continued*)

TABLE 1

(Continued)

Locus	Marker	Scaffold	Contig	PH-1[a]	00-676[b]	Missing data	χ^2	LG	Kos 3.5	LG	Kos 3.5	Hald 3.5
PAAMGA-490	AFLP			47	54	10	0.5			IIB	158.15	*197.27*
HK1215	dCAPS	2	1.150	50	61	0	1.1	3	162.42	IIB	164.39	213.20
HK731b	CAPS	2	1.150	49	62	0	1.5	3	168.47	IIB	169.55	219.04
PACMTb-400	AFLP			49	62	0	1.5			IIB	170.70	220.23
HK965	VNTR	2	1.154	55	56	0	0	3	187.48	IIB	185.08	241.35
HK1235	dCAPS	2	1.158	57	54	0	0.1	3	200.30	IIB	197.94	258.72
PACMTG-320	AFLP			52	59	0	0.4			IIB	212.60	277.62
HK1055	VNTR	2	1.159	51	60	0	0.7	3	216.75	IIB	216.19	281.42
Tri4/HK661	CAPS	2	1.159	51	60	0	0.7	3	216.75	IIB	216.19	281.42
HK1053(=HK749)	VNTR	2	1.159	51	60	0	0.7	3	225.90	IIB	224.54	291.11
5S/HK1239	CAPS	2	1.160	53	58	0	0.2	3	231.42	IIB	229.89	297.27
PAAMTT-390	AFLP			55	51	5	0.1			IIB	232.93	300.53
HK649	dCAPS	2	1.163	56	55	0	0	6	0.00	IIC	0.00	0.00
PAAMGG-220	AFLP			57	54	0	0.1			IIC	8.45	10.76
HK1057	VNTR	2	1.166	61	50	0	1.1	6	14.74	IIC	18.29	21.97
HK1263	CAPS	2	1.168	63	48	0	2	6	26.99	IIC	30.05	36.45
PAAMTT-370	AFLP			48	56	7	0.6			IIC	48.26	62.28
HK635	dCAPS	2	1.173	59	52	0	0.4	6	54.93	IIC	60.09	76.09
HK757b	CAPS	2	1.179	59	52	0	0.4	6	54.93	IIC	60.09	76.09
HK637	dCAPS	2	1.179	58	53	0	0.2	6	55.85	IIC	60.95	76.99
HK643	CAPS	2	1.183	58	53	0	0.2	6	55.85	IIC	60.95	76.99
HK551	CAPS	2	1.192	59	52	0	0.4	6	67.48	IIC	72.17	90.18
HK1115	dCAPS	2	1.192	58	53	0	0.2	6	68.36	IIC	72.87	90.97
PAAMGA-265	AFLP			63	47	1	2.3			IIC	81.68	101.22
PACMTG-750	AFLP			58	53	0	0.2			IIC	89.84	114.49
HK1149	CAPS	2	1.194	52	59	0	0.4	6	86.43	IIC	95.66	121.26
PAAMTG-270	AFLP			51	57	3	0.3			IIC	109.47	142.65
HK1343	VNTR	39	1.506	62	49	0	1.5	6	104.95	IIC	115.34	151.39
PACMTG-305	AFLP			56	55	0	0			IIC	117.57	153.58
PAAMAA-535	AFLP			58	48	5	0.9			IIC	119.34	*148.26*
HK1121	CAPS	10	1.474	56	55	0	0	6	109.61	IIC	121.59	156.08
PAAMTT-470	AFLP			49	44	18	0.3			IIC	124.12	158.87
HK1119	CAPS	10	1.473	55	56	0	0	6	113.67	IIC	126.48	161.60
HK1117	dCAPS	10	1.472	60	51	0	0.7	6	120.13	IIC	131.33	167.22
PAAMTG-515	AFLP			46	59	6	1.6			IIC	146.40	187.19
				Chromosome 3								
HK1253	CAPS	3	1.196	51	60	0	0.7	4	0.00	IIIA	0.00	0.00
HK1059	VNTR	3	1.196	60	51	0	0.7	4	22.95	IIIA	22.84	29.07
HK1265	dCAPS	3	1.196	66	45	0	4*	4	45.72	IIIA	45.73	57.92
HK1255	CAPS	3	1.197	66	45	0	4*	4	45.72	IIIA	45.73	57.92
HK973	VNTR	3	1.197	58	53	0	0.2	4	57.42	IIIA	57.30	72.67
PAAMCC-220	AFLP			62	49	0	1.5			IIIA	61.62	78.08
PAAMTG-395	AFLP			57	51	3	0.3			IIIA	69.31	87.63
Nit	Phenotype			61	50	0	1.1	4	71.47	IIIA	72.42	90.98
HK1273	CAPS	3	1.199	61	50	0	1.1	4	*77.50*	IIIA	*77.75*	*96.56*
HK375	CAPS	3	1.209	63	48	0	2	4	73.19	IIIA	73.89	92.50
HK1221	dCAPS	3	1.209	63	48	0	2	4	73.19	IIIA	73.89	92.50
HK1013	dCAPS	3	1.212	63	48	0	2	4	73.19	IIIA	73.89	92.50
HK979	VNTR	3	1.213	64	47	0	2.6	4	73.93	IIIA	74.47	93.08
HK1039	dCAPS	3	1.224	64	47	0	2.6	4	73.93	IIIA	74.47	93.08
HK1015	dCAPS	3	1.228	64	47	0	2.6	4	73.93	IIIA	74.47	93.08
HK679	dCAPS	3	1.230/1.231	64	47	0	2.6	4	73.93	IIIA	74.47	93.08
PAAMTG-550	AFLP			55	50	6	0.2			IIIA	82.27	101.64
PACMGT-530	AFLP			73	37	1	11.8***			IIIA	90.50	112.02
HK1249	FLP	3	1.258	66	45	0	4*	4	101.17	IIIA	103.00	131.06
HK891	dCAPS	8	1.452	66	45	0	4*	4	102.99	IIIA	104.85	133.13

(*continued*)

TABLE 1

(Continued)

Locus	Marker	Scaffold	Contig	PH-1[a]	00-676[b]	Missing data	χ^2	LG	Kos 3.5	LG	Kos 3.5	Hald 3.5
HK947	dCAPS	8	1.454	66	45	0	4*	4	102.99	IIIA	104.85	133.13
HK1209	dCAPS	8	1.456	64	47	0	2.6	4	104.71	IIIA	106.60	135.03
PAAMTG-175	AFLP			59	49	3	0.9			IIIA	107.89	136.35
PAAMGG-560	AFLP			57	51	3	0.3			IIIA	112.11	141.02
HK1323	VNTR	8	1.458	69	42	0	6.6*	4	115.18	IIIA	119.08	149.39
PACMCC-220	AFLP			57	52	2	0.2			IIIB	0.00	0.00
PAAMGG-620	AFLP			46	60	5	1.9			IIIB	16.41	22.64
HK1279	CAPS	8	1.461	59	52	0	0.4	9	*2.62*	IIIB	*28.79*	*37.20*
HK1187	CAPS	26	1.492	60	51	0	0.7	9	0.00	IIIB	25.70	33.92
HK1135	CAPS	26	1.492	59	52	0	0.4	9	0.91	IIIB	28.21	36.58
PAAMTG-90	AFLP			56	52	3	0.1			IIIB	29.88	38.34
PACMTT-450	AFLP			61	50	0	1.1			IIIB	33.63	42.46
PAAMCA-405	AFLP			56	53	2	0.1			IIIB	40.13	50.20
HK927	CAPS	9	1.464	64	47	0	2.6	9	19.38	IIIB	47.56	59.81
PAAMCA-125	AFLP			63	47	1	2.3			IIIB	51.24	64.08
PAAMAA-90	AFLP			62	45	4	2.7			IIIB	62.35	77.85
PAAMCC-320	AFLP			59	52	0	0.4			IIIB	78.70	99.10
HK939	dCAPS	9	1.467	59	52	0	0.4	12	0.00	IIIB	90.94	113.33
PACMGT-590	AFLP			76	34	1	16***			IIIB	113.79	145.97
					Chromosome 4							
HK1189	Plus/minus	27	1.493	42	69	0	6.6*	13	0.00	IVA	0.00	0
PACMGT-185	AFLP			51	59	1	0.6			IVA	8.39	9.218
PACMTT-325	AFLP			57	54	0	0.1			IVA	24.05	33.948
HK1063	VNTR	4	1.259	52	59	0	0.4	7	0.00	IVA	30.94	42.088
HK675	dCAPS	4	1.259	57	54	0	0.1	7	4.83	IVA	35.49	47.625
HK1097	dCAPS	4	1.280	62	49	0	1.5	7	17.35	IVA	47.41	62.735
HK1067	VNTR	4	1.296	60	51	0	0.7	7	20.78	IVA	50.79	66.577
HK1009	dCAPS	4	1.298	61	50	0	1.1	7	21.69	IVA	51.70	67.571
HK755	CAPS	4	1.300	62	49	0	1.5	7	22.56	IVA	52.53	68.461
HK935	dCAPS	4	1.302	64	47	0	2.6	7	24.33	IVA	54.28	70.344
Hyg	Phenotype	4	1.304	63	48	0	2	7	24.70	IVA	54.63	70.708
HK461	CAPS	4	1.309	63	48	0	2	7	25.48	IVA	55.41	71.56
HK1011	dCAPS	4	1.313	62	49	0	1.5	7	28.03	IVA	57.94	74.36
HK887	CAPS	4	1.314	59	52	0	0.4	7	32.55	IVA	62.34	79.45
PACMCC-410	AFLP			55	54	2	0			IVA	74.77	95.87
HK1267	dCAPS	4	1.316	54	57	0	0.1	7	46.79	IVA	77.21	98.55
HK1257	CAPS	4	1.316	51	60	0	0.7	7	55.67	IVA	85.47	108.81
HK1251	dCAPS	4	1.318	47	64	0	2.6	7	70.11	IVA	97.58	124.64
PACMGT-225	AFLP			46	64	1	3			IVA	109.91	141.18
PAAMCA-225	AFLP			44	65	2	4*			IVA	114.80	146.46
PACMTG-175	AFLP			44	67	0	4.8*			IVA	122.54	155.50
PAAMTG-160	AFLP			59	48	4	1.1			IVA	141.99	185.89
HK633	dCAPS	4	1.320	60	51	0	0.7	5	0.00	IVA	147.16	192.34
HK1283	dCAPS	4	1.322	55	55	1	0	5	9.40	IVA	155.99	203.30
HK943	dCAPS	6	1.401	56	55	0	0	5	12.21	IVA	158.74	206.42
HK949	dCAPS	6	1.399	55	56	0	0	5	13.12	IVA	159.64	207.43
HK1073	VNTR	6	1.398	55	56	0	0	5	13.12	IVA	159.64	207.43
HK673	dCAPS	6	1.395	53	58	0	0.2	5	14.95	IVA	161.46	209.44
TUB/HK1023	dCAPS	6	1.393	54	57	0	0.1	5	15.86	IVA	162.37	210.46
HK1021	dCAPS	6	1.391	54	57	0	0.1	5	15.86	IVA	162.37	210.46
HK1127	dCAPS	15	1.479	56	55	0	0	5	19.50	IVA	165.96	214.49
HK1071	VNTR	6	1.384	57	54	0	0.1	5	20.32	IVA	166.79	215.42
HK1019	dCAPS	6	1.383	56	55	0	0	5	21.16	IVA	167.64	216.36
HK1137	dCAPS	33	1.499	56	55	0	0	5	22.39	IVA	168.80	217.64
HK1281	dCAPS	41	1.508	62	49	0	1.5	5	24.34	IVA	170.73	219.75
HK1017	dCAPS	6	1.373	55	56	0	0	5	26.64	IVA	172.95	222.31

(*continued*)

TABLE 1

(Continued)

Locus	Marker	Scaffold	Contig	PH-1[a]	00-676[b]	Missing data	χ^2	LG	Kos 3.5	LG	Kos 3.5	Hald 3.5
HK299	CAPS	6	1.372	57	54	0	0.1	5	28.46	IVA	174.76	224.37
HK629	FLP	6	1.371	57	54	0	0.1	5	30.32	IVA	176.57	226.42
HK1211	dCAPS	6	1.371	57	54	0	0.1	5	30.32	IVA	176.57	226.42
PAAMTG-320	AFLP			58	50	3	0.6			IVA	190.04	243.42
PAAMGA-112	AFLP			71	39	1	9.3**			IVB	0.00	0.00
PACMGT-285	AFLP			53	57	1	0.1			IVB	18.10	22.57
HK717	CAPS	6	1.367	50	61	0	1.1	8	0.00	IVB	20.28	24.83
HK205	dCAPS	6	1.367	50	61	0	1.1	8	0.00	IVB	20.28	24.83
IGS/HK665	dCAPS	6	1.364	50	61	0	1.1	8	0.00	IVB	20.28	24.83
HK235	dCAPS	Unknown	No hit	50	61	0	1.1	8	0.00	IVB	20.28	24.83
PAAMCC-620	AFLP			49	61	1	1.3			IVB	21.38	25.95
PAAMGA-110	AFLP			52	58	1	0.3			IVB	24.76	29.63
PAAMCC-110	AFLP			51	60	0	0.7			IVB	33.39	39.85
PAAMTG-505	AFLP			60	45	6	2.1			IVB	40.47	48.07

Sequence-tagged site (STS) markers were arranged according to both physical position, derived from whole-genome sequencing, and genetic map. AFLP markers were ordered according to placement in the genetic map on the basis of the Kosambi mapping function, using JoinMap at LOD 3.5. Italic values indicate either disagreement with the physical map or discrepancies between maps generated by the different mapping functions [Kosambi (Kos) *vs.* Haldane (Hald)]. Significant segregation distortions are indicated with $*P < 0.05$, $**P < 0.01$, and $***P < 0.001$. Linkage groups (LG) are given for map analysis using the Kosambi mapping function at LOD 3.5 using STS markers alone and for the final map that also includes AFLP markers using both the Kosambi and Haldane mapping functions at LOD 3.5. Map distances are given in centimorgans.

[a] Progeny with PH-1-type alleles.

[b] Progeny with 00-676-type alleles.

than the smaller scaffolds being contained within scaffold 5, it follows that the map position of HK663 was in error. An identical situation was encountered concerning the placement of HK1279 that was sequence tagged to the end of scaffold 8. Scaffold 26 overlapped with scaffold 30, forming a combined scaffold measuring 14,036 bp. Two markers were located on scaffold 26 that mapped within scaffold 8 before HK1279. Again, we assume an erroneous map position for HK1279 to place scaffolds 26/30 between scaffolds 8 and 9.

Scaffolds 15 (9308 bp), 33 (6569 bp), and 41 (4810 bp) all mapped to scaffold 6 (Table 1). In these instances, map distances to regions between scaffolds are too substantial for mapping problems to be a possible issue. Therefore, we suppose that the map positions of these scaffolds are accurate and that the placement of these smaller scaffolds may be between adjacent contigs of a scaffold or otherwise reflects errors in the sequence assembly for these regions of the genome.

The locus containing the hygromycin resistance marker within the *Fst12* gene was incorrectly placed in initial genetic maps, mapping ~25 cM from its expected position. Visual examination of the haplotype map revealed a large number of single-locus double crossovers to adjacent markers in this genomic region that otherwise displayed little recombination. The hygR phenotype also did not meet Mendelian expectation for 1:1 segregation ($P = 0.008$) due to an excess of drug-sensitive progeny. This suggested that a number of progeny were scored as drug sensitive due to incomplete penetrance of the drug resistance phenotype. To test this possibility, all 23 drug-sensitive progeny for which single-locus double crossovers were invoked were tested for the presence of the *hph* gene. PCR analysis of these 23 progeny using primers that amplify an internal fragment of *hph* indicated that all progeny in question carried the gene. Additional testing on hygromycin-amended plates, however, confirmed that each culture was indeed hygromycin sensitive. Sequence analysis of *hph* for two of these progeny revealed six point mutations each in the 312 bp fragments sequenced. Mutations were consistent with C to T transitions, suggesting that repeat-induced mutations (RIP) (Galagan and Selker 2004) may have caused gene inactivation in the 23 strains in question. As RIP affects duplicated or repetitive sequences, we suggest that initial transformation of PH-1 may have included more than one copy of *hph*, perhaps as a tandem repeat. The data were adjusted for the 23 progeny to reflect the presence of the *hph* sequence and not the expression of the phenotype. The modified data resulted in a locus mapping to a position consistent with the *Fst12* locus and the previously observed segregation distortion for this locus disappeared ($P = 0.155$).

Three markers (one dCAPS, twoVNTRs) were not used for final map analyses. HK1285 (dCAPS marker), which was designed to and connected the two linkage groups in scaffold 2, was removed as its inclusion led to a significant disturbance of map order across the

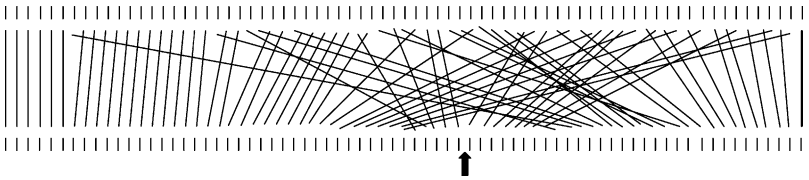

FIGURE 1.—Illustration of a map disturbance caused by a single marker. HK1285, a sequence-tagged marker at contig 1.161 in scaffold 2, brought together two large linkage groups (positioned to the right and left of the arrow that indicates physical position of this marker). However, inclusion of HK1285 changed the map order of STS and AFLP markers from their (correct) positions in the bottom row to the order indicated in the top row.

two linkage groups (Figure 1). Two VNTR markers, one (HK1335) connecting the two linkage groups in scaffold 6 and another (HK1371) positioned in scaffold 3, also were removed, as their inclusion led to exclusion of other markers. In both instances, JoinMap, while placing the two VNTR markers at correct physical positions, was unable to integrate all other loci (*i.e.*, some loci remained ungrouped) in the mapping groups in question without having to greatly relax the mapping parameters.

After adjustments were made to the STS marker data set, data from the 80 AFLP markers were included in linkage analyses. Two markers, PAAMCC-118 and PAAMCC-110, were found to have generated identical data and one marker, PAAMCC-118, was discarded, leaving 79 AFLP markers. Of these, 5 did not group with any other marker after linkage analysis. As all 5 markers showed segregation distortions with χ^2-values of 8.2–63.2, they were discarded. One additional AFLP marker was excluded due to a χ^2-value of 59.1. Two AFLP markers disturbed the map, although neither one displayed segregation distortion. The map disturbance was local and affected the placement of ~10 other loci over a span of ~30–40 cM.

A final evaluation of the placement of AFLP markers was done visually with the help of the haplotype map (Figure 2) containing the raw data. Five AFLP markers that were forced into the map in the third round were discarded as too many single-locus double crossovers had to be invoked if these markers were placed correctly. All 5 markers also generated a high mean χ^2-contribution to the linkage group, confirming their poor fit. The remaining 66 AFLP markers were used for final map construction.

Final map construction: Using the trimmed data set, we constructed a genetic map of *F. graminearum* consisting of 235 markers. Once AFLP markers were included, the number of linkage groups was reduced from 13 to 9, at LOD 3.5 (Table 1). This LOD was chosen as it produced the minimum number of linkage groups, while maintaining the integrity of the map.

AFLP markers added significantly to map size; using the Kosambi mapping function at LOD 3.5 the map size increased from 900 to 1234 cM. When using the Haldane function the total map size increased to 1565 cM (Table 1). These increases are explained by the map location of many AFLP markers. Nearly half of the AFLP markers (43.9%) either mapped to ends of the final

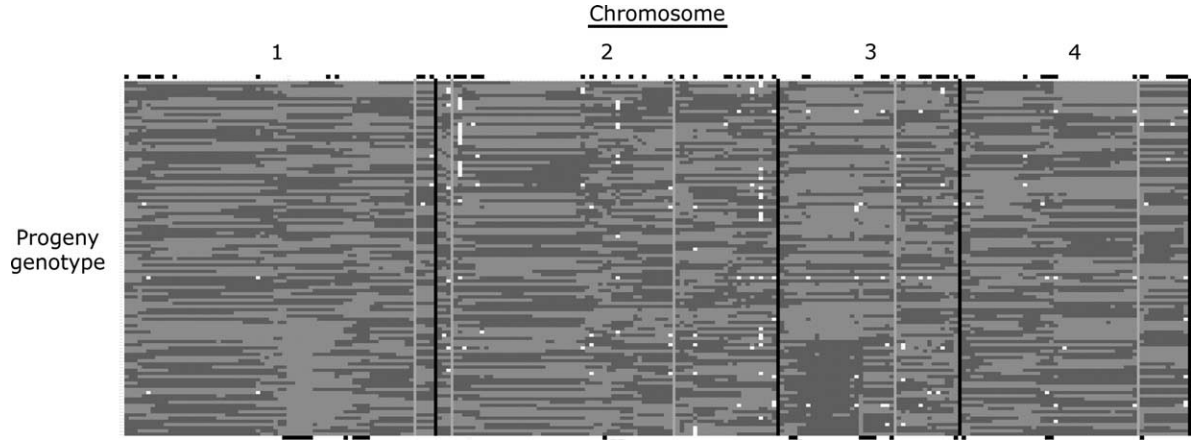

FIGURE 2.—Haplotype map for all progeny across the four chromosomes of *F. graminearum*. Boxes depict the order of genetic markers (left to right) across each chromosome: boxes with light shading indicate PH-1-type alleles, boxes with dark shading indicate 00-676-type alleles, and open boxes indicate missing data. Solid vertical lines indicate chromosomal boundaries, while vertical lines with light shading delineate the linkage groups. Solid boxes below the data indicate loci with significant segregation distortion, while solid boxes above the data show mapped locations of AFLP markers. Visual representation of data facilitated subjective decisions in favor of removal of loci accepted only in third-round mapping (forced integration), especially when displaying a substantial number of single-locus double crossovers.

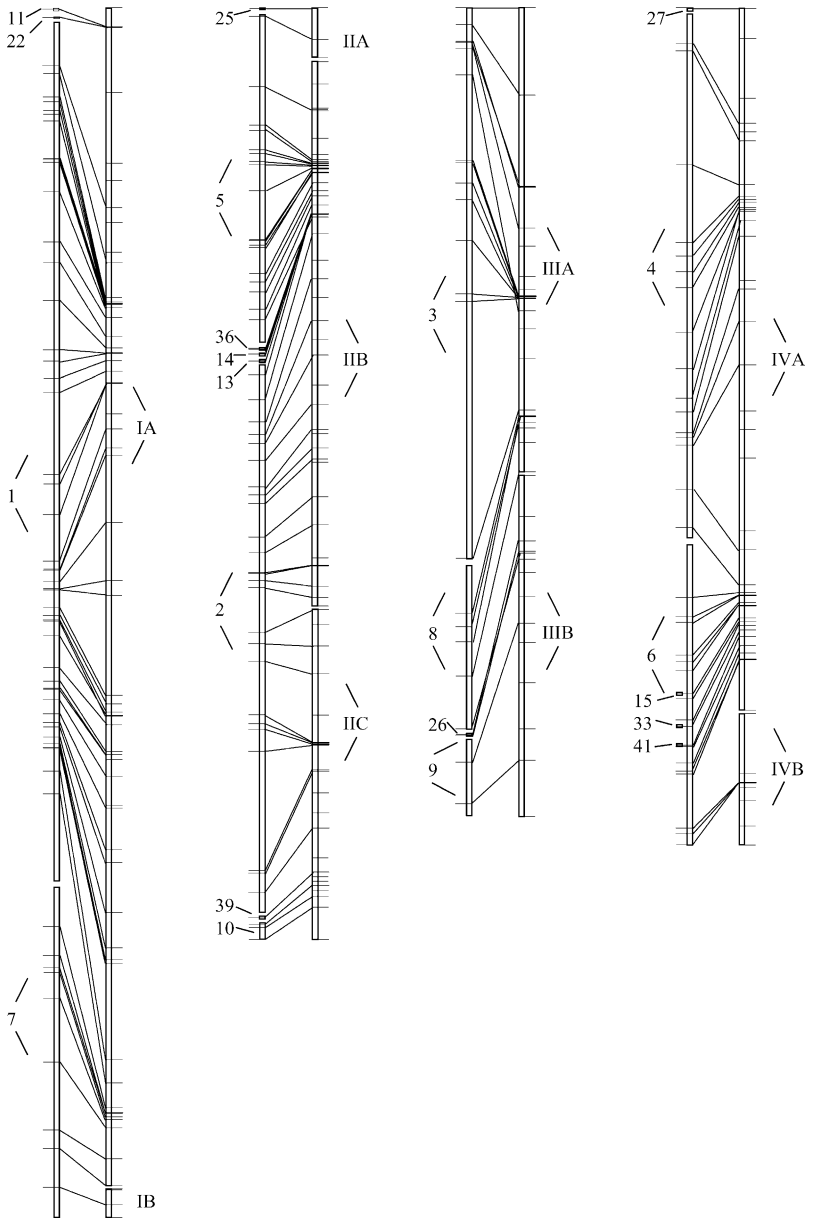

FIGURE 3.—Sketch of the alignment of physical and genetic maps resulting in chromosome maps for *F. graminearum*, adapted and modified from the maps presented at http://www.broad.mit.edu. Scaffolds integrated into the chromosome maps are indicated to the left of the four chromosomes. Thicker lines on the genetic map indicate map positions occupied by more than one marker. Linkage groups are represented as Roman numerals to the right of each chromosome map. Chromosome maps are scaled to represent the relative physical lengths of the chromosomes. The full genetic map may be found at http://www.broad.mit.edu/annotation/fungi/fusarium/markers/html.

linkage groups or were placed within previously separated linkage groups of the map based on STS markers. AFLP markers that were placed internally in existing linkage groups did not change the genetic distance previously determined by STS markers (Table 1), substantiating the accuracy of AFLP markers included in this map. Incongruence between physical and genetic map placement for markers HK663 and presumably HK1273 and HK1279 persisted after addition of AFLP markers and when using the Haldane mapping function.

Delineating chromosomes by mapping and cytology: Combining the physical and genetic maps of *F. graminearum* resulted in four clusters of scaffolds joined by genetic linkage groups (Table 1 and Figure 3) corresponding to four chromosomes. The four largest scaffolds (scaffolds 1–4) were each placed on individual chromosomes that were named accordingly (1–4). Scaffolds and linkage groups contained in the chromosomes are detailed in Table 2.

Chromosome specimens prepared by the GTBM were stained with DAPI to yield clear fluorescent images of mitotic metaphase chromosomes of both parents as shown in Figure 4. Sister chromatids were not discerned, due to the resolution limit of microscopy and the innate nature of mitotic chromosomes of filamentous fungi as revealed by electron microscopy (TSUCHIYA *et al.* 2004). Chromosome counting for PH-1 and 00-676 unambiguously showed that the genome of *F. graminearum* consists of four chromosomes, which is congruent with the combined result from physical and genetic mapping. No other chromosomes were found.

The chromosomes of *F. graminearum* were conspicuously large for the genus Fusarium. For example, even the smallest chromosome of PH-1 had a much larger

TABLE 2

Integration of physical and genetic maps of *Fusarium graminearum* into chromosome maps

Chromosome	Length (bp)	Order and orientation of scaffolds across chromosomes[a]	Linkage groups	cM[b]
1	11,588,431	(11, 22), [21*, 19*, 1], 7	IA, IB	370.09 (466.56)
2	8,840,881	25, 5, (36, [28*, 24*, 14], [13, 29*, 31*]), 2, [39, 37*], 10{−}	IIA, IIB, IIC	400.53 (512.02)
3	7,687,128	3, 18*, 8, 30*, 26, 9, 43*	IIIA, IIIB	232.87 (295.36)
4	7,893,678	27, 4, [6{−}, 34*], 15, 33, 41	IVA, IVB	230.51 (291.49)
Total	36,010,118[c]			1234 (1565.43)

[a] Scaffolds indicated by * were integrated into the chromosome complement not by genetic mapping but by sequence overlaps with other scaffolds that were not recognized by the sequence assembly program ARACHNE, but were later identified by BLAST and manual sequence assembly analyses (Sequencher 4.1.2). Scaffolds integrated by this process are indicated by [ ]. Actual order of scaffolds in parentheses () is unknown. Scaffolds followed by {−} were determined to be oriented inverse to the sequence assembly. Sequence orientation as compared to the assembly could not be determined for scaffolds (11–43), except for scaffolds overlapping with other scaffolds, indicated by [ ]. Scaffolds 15, 33, and 41 of chromosome 4 are most likely contained within scaffold 6; scaffold 43 is part of scaffold 9 according to manual sequence assembly.

[b] Map distances were determined in JoinMap 3.0 using the Kosambi and the Haldane (in parentheses) mapping functions.

[c] Covers all nuclear sequences generated by shotgun whole-genome sequencing, except for five scaffolds (59,630 bp).

axis length (~7 μm in Figure 4) than the longest chromosome of *F. solani* (~3.6 μm) (Taga *et al.* 1998). In addition, constrictions reminiscent of centromeres were present in each chromosome, and a faintly stained projection of loosened chromatin extending from the end of one chromosome was constantly observed in the specimens representing metaphase. On the basis of evidence obtained for other filamentous ascomycetes by fluorescence *in situ* hybridization (FISH) (Taga and Murata 1994; Taga *et al.* 2003), this protrusion is thought to be a nucleolus organizer region (NOR), *i.e.*, rDNA.

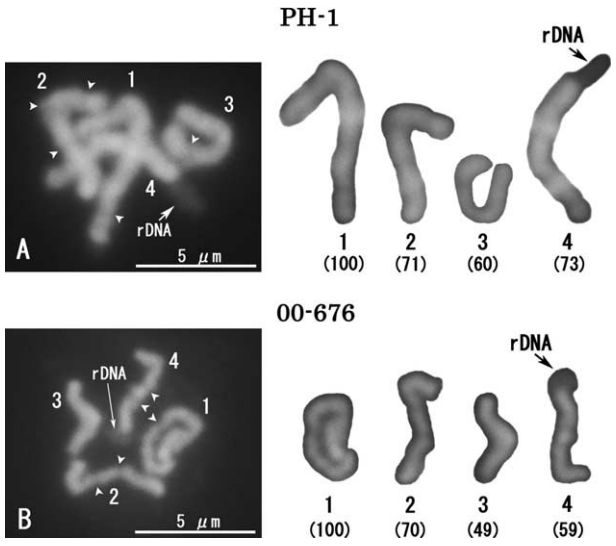

Figure 4.—Fluorescence images of mitotic metaphase chromosomes of strains PH-1 (A) and 00-676 (B) of *F. graminearum* and alignment of individual chromosomes. Chromosomes are numbered according to the results from physical and genetic mapping. Numbers in parentheses below the aligned chromosomes indicate the length relative to the longest one (chromosome 1), which was designated as 100. Arrow heads indicate position of chromosome constrictions.

Although the absolute size of chromosome complements varied with specimens, longitudinal size-based alignment of the chromosomes was possible for each specimen in the two strains (Figure 4). Summarizing the data for several specimens of good quality in both strains (data not shown), the four chromosomes consist of one that is by far the longest and three smaller ones. Among the latter, constant size-based ordering was difficult due to the variance of samples and small differences in size among the three chromosomes. Without taking into account the size of rDNA, the NOR chromosome was the second or third largest in both strains.

Segregation distortion: Significant segregation distortion that departed from Mendelian expectation at $P = 0.05$ was observed for 25 loci in the final map (19 STSs, 6 AFLP markers; 25/235 = 10.6%) (Table 1 and Figure 2). A significant cluster of loci with segregation distortion, consisting solely of STS markers, was observed in scaffold 1 spanning 829 kb between contigs 1.93 and 1.110 (based on 7 mapped STS loci). The gene encoding nitrate reductase (*Nit*1) is situated roughly in the middle of this cluster within contig 1.104 (position 58,293–61,593 bp). The STS marker closest to the genomic location of *Nit*1 was HK607, ~73 kb and 2 cM away.

Biased representation of nit1 progeny in the mapping population could account for the first area of segregation distortion. The nit1 and nitM phenotypes are conferred by genes at two loci. The *Nit*1 locus corresponds to the structural gene for nitrate reductase while NitM corresponds to an uncharacterized and unlinked gene. The nitM phenotype is epistatic to the nit1 phenotype, and progeny consisted of ascospore cultures with nitM, nit1, and WT phenotypes in proportions that were not significantly different from the expected 2:1:1. Nevertheless, a slight excess of nitM and WT progeny was found when the observed proportion of 61:21:30

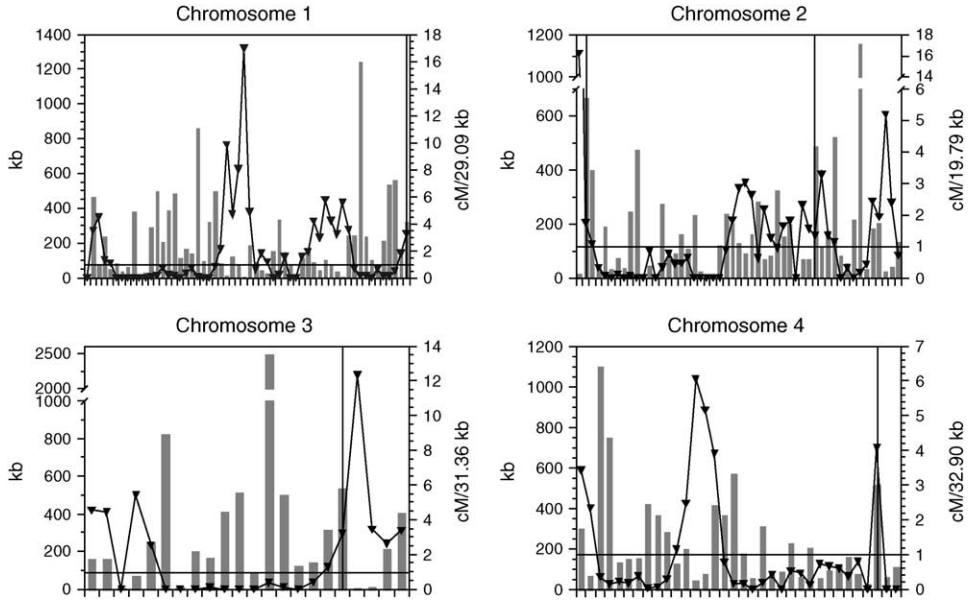

FIGURE 5.—Physical distances between sequence-tagged site markers (columns) and relative map distances between them, standardized to the average distance per centimorgan for the four chromosomes of *F. graminearum*. The average of 1 cM/*x* kb across the individual chromosomes is indicated by a horizontal line; linkage group gaps are depicted by vertical lines.

(nitM:*nit*1:WT) was compared to the expected proportion of 56:28:28. WT progeny were wild type at the *Nit*1 locus (the allele in the parent PH-1), and half of the nitM progeny were expected to be *Nit*1 also. When data for the nit phenotype were compared side by side with the data from the closely linked locus defined by HK607 it became clear that the *nit*1 allele among nitM ascospores likely was more infrequent than expected. On the basis of data from locus HK607, 39 nitM progeny were scored as having a PH-1-type allele (and therefore were presumably *Nit*1) and only 22 progeny displayed a 00-676-type and presumably the *nit*1 allele. If these data are evaluated together with the slight deficiency of *nit*1 mutants in the original scoring process ($22 + 21 = 43$ *nit1* progeny:68 *Nit1* progeny) one could conclude that *nit1* progeny were inadvertently undersampled ($P < 0.02$) during the progeny selection process, possibly due to poor growth in the initial stages of development (ascospore progeny were isolated soon after germination).

A second cluster of loci with segregation distortion on the same scaffold involving five loci was observed between contigs 1.114 and 1.116 (along 260 kb). Due to a significant genetic distance of ~50 cM to the *Nit*1 locus, selection at *Nit*1 was not responsible for the segregation distortion in this genomic region, even though an excess of PH-1-type alleles was again observed (Table 1).

A third cluster of segregation distortion spanned the ends of scaffolds 3 and 8 in linkage group 5, covering at least 612 kb. χ^2-values, although significant, were lower than those for the above-mentioned clusters, with the exception of an AFLP marker with a χ^2-value of 11.8. Finally, a fourth area involved two markers in scaffold 3, HK1265 and HK1255, with both being just significant, spanning a region of 3 kb. These four areas accounted for 18 of the 25 markers (72%) with segregation distortion.

Genomic location of NitM: Segregation of the NitM phenotype was not significantly different from Mendelian expectation: 61 progeny were nitM (PH-1 type) and 50 progeny were non-nitM (*nit*1 mutants or WT, nitM being epistatic to nit1). NitM mapped to scaffold 3 within linkage group 5 (Table 1). Excluding HK1273, which was slightly out of order, the physical location of the *NitM* locus was predicted to be on contig 1.206, assuming a linear relationship between physical and genetic map between contigs 1.197 and 1.209. As NitM has been proposed to result from a gene for a molybdenum cofactor protein, a search was performed for such proteins at the *F. graminearum* database webserver (http://mips.gsf.de) of the Munich Information Center for Protein Sequences (MEWES *et al.* 2004). Among four matches, one of the predicted proteins (FG05028) was located in scaffold 3, contig 1.202, close to the predicted linear position of *NitM*. We postulate that this gene determined the NitM phenotype. As recombination rates were higher at the beginning of linkage group 5 and were very low distal to the putative *NitM* locus, a linear relationship between physical and genetic distance is unlikely, supporting the proposed identity of FG05028 and *NitM*. This proposal now can be tested by site-directed mutagenesis.

Relationship between physical and genetic distance: The average spacing of genetic markers among anchored scaffolds was calculated to be 153 kb, though the distance between STSs varied considerably. We normalized physical to genetic map distance between markers, on the basis of the average DNA length between STS markers/centimorgans within each chromosome to adjust for that variability. Therefore, values >1 would indicate a higher than average recombination rate, while values <1 would indicate a lower than average recombination rate between STS markers. In Figure 5, peaks in

the line representing these values indicate genomic regions with relatively high recombination whereas other regions display relatively little recombination. Briefly, in chromosome 1, a region at the beginning of the chromosome with high recombination is followed by a genomic region >4 Mb with little or no recombination flanked by markers HK1271 and HK1231. This region physically covers about one-third of chromosome 1 but contributes only 24 cM (of 370 cM = 6.5%) to the map size of this chromosome. A 500-kb region follows with recombination rates higher than average between HK931 and HK1293. Further along the chromosome a 750-kb region between HK693 and HK961 is observed with high recombination rates, followed by 3.3 Mb with lower than average recombination rates. In chromosome 2, 1 Mb with high recombination rates (between HK1185 and HK1219) is followed by 2.5 Mb with lower than average recombination rates (between HK1219 and HK1049). The remainder is recombinationally active, except for a region of 1.5 Mb between HK635 and HK1115. Chromosome 3 displayed higher than average recombination rates at the two chromosome ends. In contrast, an ~2-Mb region located between HK1273 and HK679 displayed low recombination rates. Two recombinationally active regions characterize chromosome 4, one being located between HK1011 and HK633 covering ~860 kb and the other being observed between HK1211 and HK717.

Map on the web: More details regarding this map, including a FASTA file of all sequence-based markers, can be found at http://www.broad.mit.edu/annotation/fungi/fusarium/maps.html and at the NCBI website at http://www.ncbi.nlm.nih.gov/mapview/map_search.cgi?taxid=229533. Genetic markers may be viewed within the genome browser of FGDB at http://mips.gsf.de/genre/proj/fusarium/.

DISCUSSION

Using a combination of primarily STS and AFLP markers (totaling 235 markers), we were able to generate a high-quality genetic map of *F. graminearum* consisting of nine linkage groups that covers 36 Mb or 99.83% of the draft sequence assembly of the nuclear genome of *F. graminearum*. The genetic map made it possible to order most scaffolds generated by shotgun whole-genome sequencing, and vice versa, the linkage groups were organized with the help of the physical map. As a consequence all linkage groups and most scaffolds were incorporated into four chromosomes.

A chromosome number of four for *F. graminearum* was first reported by Howson *et al.* (1963), using a conventional squash technique on meiosis. However, results from such conventional cytology, especially those for Fusarium spp., have been shown to be generally unreliable (Taga *et al.* 1998). Later, $n = 4$–5 for Japanese isolates of *F. graminearum* were observed on the basis of GTBM (T. Sato, M. Taga and H. Saitoh, unpublished observations). When these results are considered in conjunction with the recent determination of species limits within the Fg species complex (O'Donnell *et al.* 2004), and bearing in mind the ubiquitous occurrence of karyotype polymorphism in filamentous fungi (Kistler and Miao 1992; Zolan 1995), a chromosome number of $n = 4$ could not be assumed *a priori* for the strains used in this study. Cytological analysis unambiguously confirmed the conclusion from the genetic linkage analysis for chromosome number, showing the power of cytology in combination with genetic mapping for resolving chromosome number. By comparing characteristics of the four chromosomes such as length and location of rDNA generated by physical and genetic mapping, we were able to match them with chromosomes observed cytologically without the use of FISH.

We could not detect distinct differences in morphological features of chromosomes between PH-1 and 00-676 in this study. However, future studies are needed to clarify if their chromosomes contain structural rearrangements that may have caused distorted segregation of markers or suppressed recombination observed in this study. Especially important to consider would be the suppressed recombination along a 2-Mb region of chromosome 3. Such suppression may be caused by an inversion and should be analyzed by meiotic cytogenetics incorporating pachytene analysis.

Graphical display of standardized map distances across the chromosomes (Figure 5) allows for an understanding of existing linkage group divisions. Without exception, all linkage gaps represent regions of higher than average recombination. Integrating whole chromosomes into single linkage groups may require more detailed analyses in these genomic regions, using several additional markers. The effects of HK1285 illustrate potential mapping problems. This marker is positioned between two markers placed in different linkage groups that together define most of chromosome 2. Integration of HK1285, although connecting the linkage groups, changes the map order over much of this region. Recombination rates in this genomic region are probably very high, necessitating high-resolution mapping to maintain integrity of the genetic map.

Five smaller scaffolds of nuclear origin remained unmapped, *i.e.*, scaffolds 12 (10,493 bp), 16 (9291 bp), 32 (6728 bp), and 35 (6025 bp) and one scaffold that originally consisted of four scaffolds (40, 38, 17, and 20) but could be integrated (by considering sequence overlaps) into one scaffold of 27,093 bp. GC content in these five scaffolds was lower than the average of 48.3% and ranged between 35.9 and 47.2%. No polymorphisms were identified in these scaffolds despite sequencing substantial portions for 00-676 and exploring a number of VNTR loci. The inability to identify polymorphisms in certain genomic regions illustrates the main challenge

of this mapping project: modest levels of polymorphisms between the parents. PH-1 and 00-676 appear to be very closely related [see O'Donnell *et al.*'s (2004) Figure 6: phylogram of 11 combined genes]. Population genetic analysis indicates that Midwestern U.S. populations of *F. graminearum* are outcrossing (L. R. Gale, unpublished results; Zeller *et al.* 2004). Therefore, any two isolates randomly selected from that region would generate equally only modest amounts of polymorphisms. Low diversity within U.S. populations of *F. graminearum* has been noted before, especially when compared to other fungi (L. R. Gale, unpublished results; Gale *et al.* 2002). Nevertheless, there is evidence that *F. graminearum* populations are subdivided and a population of *F. graminearum* that is genetically divergent from the resident U.S. population has been identified in Minnesota and North Dakota (L. R. Gale, unpublished results). Future crosses to establish additional and more detailed maps, *e.g.*, to integrate the remaining scaffolds, to examine in detail the regions between linkage groups and the regions of high recombination rates should take advantage of this higher level of diversity between isolates of these subpopulations. Ideally, derivatives of PH-1 should serve as one of the parents, as the genome sequence is available for this strain.

For future genetic analysis, VNTRs are the most efficient and economical markers and perform very reliably. In addition, VNTRs are sequence tagged and can be designed easily and polymorphisms can be assessed directly after PCR on gels. Development of SNPs requires sequencing of the other parent and evaluation of SNPs often requires the development of a second primer pair (for dCAPS analysis), in addition to restriction enzyme digestion. Some of the difficulties in developing markers for genetic analysis from SNPs may be alleviated soon. Syngenta (Wilmington, DE) recently released a *F. graminearum* genome sequence based on strain GZ3639 (NRRL 29169), another strain originally isolated from the Midwestern United States and closely related to PH-1 and 00-676. The Broad Institute currently handles this sequence and will identify SNPs between PH-1 and GZ3639. Depending on coverage and quality of this additional genome sequence and on extent and genomic locations of SNPs identified from the two sequences, progeny from a cross between PH-1 and GZ3639 could be used to further address issues raised by this study once the second genome sequence is released to the public.

Finally, AFLP is an efficient technique for generating large numbers of markers and AFLP markers have been valuable in this project to connect linkage groups. They often mapped in groups in regions not well represented by STS markers. Integration of AFLP markers into genetic maps, though, can be problematic, especially in the absence of STS markers.

On the basis of a multilocus species level phylogeny (O'Donnell *et al.* 2004), the previously published genetic map of *F. graminearum* was derived from an interspecific cross between *F. graminearum* and *F. asiaticum* (Jurgensen *et al.* 2002). Nevertheless, the following results of Jurgensen *et al.* (2002) were confirmed by our current study: (1) the same number of linkage groups (nine); (2) the linking of scaffolds (3, 8, 9), (4, 6), and (1, 7) into separate linkage groups, although the orders of scaffolds 8 and 9 are different in the two maps; and (3) estimates of total map size based on the Kosambi mapping function were very similar (1300 *vs.* 1234 cM). However, other characteristics of the map by Jurgensen *et al.* (2002) appear to reflect differences between using an interspecific *vs.* an intraspecific cross and the maps resulting from them. These include recombination suppression in four linkage groups based on the observation that half of the progeny did not show any crossovers in these linkage groups, chromosomal rearrangements (inversions) in two linkage groups, and significant segregation distortion in five of the nine linkage groups (Jurgensen *et al.* 2002).

Intriguingly, little or no recombination was observed over long sections ($\geq$1 Mb) across the chromosomes of *F. graminearum*, followed by regions often spanning several hundred kilobases that displayed considerably higher than average recombination rates. The terms recombination hotspots and coldspots are generally reserved to indicate small genomic regions, with hotspots that display high densities of crossing over often being present only within a genomic region of just a few kilobases (*e.g.*, Gerton *et al.* 2000; De Massy 2003). As we identified regions in our genetic map spanning several hundred kilobases with recombination rates lower or higher than average, the terms hotspots and coldspots probably should not be applied for our system.

Information on the distribution and orientation of scaffolds on the four chromosomes, together with the assessment of recombination rates across the four chromosomes, will be an invaluable resource for population genetic analysis of *F. graminearum*. STS markers now can be chosen judiciously depending on the objective of a particular study. If markers are needed for an unbiased view of recombination at a population level, ones can be chosen that are appropriately spaced within chromosomes or are from different chromosomes to avoid problems with linkage disequilibrium. On the other hand, this map is based on the progeny of a single perithecium. A different view concerning rates of recombination within chromosomes may be gained if evaluated at the population level. For example, if markers are chosen from genomic regions that are physically close, recombination rates between loci can be indirectly assessed by levels of gametic disequilibria between them (Nachman 2002). Prospects for and challenges to the estimation of recombination rates with a population genetics approach have been reviewed recently (Stumpf and McVean 2003). The chromosome maps and the markers developed in this study could serve as a

foundation for a population genomics approach that links genomics and population genetics. Such a study may reveal loci under selection or help to understand evolutionary processes affecting genome heterogeneity such as gene flow or random genetic drift (Luikart *et al.* 2003).

The authors thank our collaborators at the Broad Institute, including Bruce Birren, Christina Cuomo, and Li-Jun Ma for their continued interest and support of Fusarium genomics. Karen Hilburn and Sam Gale, U.S. Department of Agriculture, Agricultural Research Service, Cereal Disease Laboratory, St. Paul, Minnesota are thanked for outstanding technical support and Jacki Morrison is thanked for help with graphics. This work was carried out in part using computing resources at the University of Minnesota, Supercomputing Institute. We acknowledge the continued support of the U.S. Wheat and Barley Scab Initiative; funding for the genetic map project by the State of Minnesota Rapid Response Fund; and funding for the genome sequence of *F. graminearum* provided by the U.S. Department of Agriculture, Cooperative State Research Education and Extension Service, Microbial Genome Sequencing Project, award no. 2002-35600-12782. M. Taga was financially supported in part by a grant-in-aid for scientific research from the Japan Society for the Promotion of Science (16580029) and by the Okayama University Center of Excellence program "Establishment of Plant Health Science."

LITERATURE CITED

Batzoglou, S., J. B. Jaffe, K. Stanley, J. Butler, S. Gnerre *et al.*, 2002 ARACHNE: a whole-genome shotgun assembler. Genome Res. **12:** 177–189.

Benson, G., 1999 Tandem repeats finder: a program to analyze DNA sequences. Nucleic Acids Res. **27:** 573–580.

Bowden, R. L., and J. F. Leslie, 1992 Nitrate-nonutilizing mutants of *Gibberella zeae* (*Fusarium graminearum*) and their use in determining vegetative compatibility. Exp. Mycol. **16:** 308–315.

Bowden, R. L., and J. F. Leslie, 1999 Sexual recombination in *Gibberella zeae*. Phytopathology **89:** 182–188.

Correll, J. C., C. J. R. Klittich and J. F. Leslie, 1987 Nitrate nonutilizing mutants of *Fusarium oxysporum* and their use in vegetative compatibility. Phytopathology **77:** 1640–1646.

De Massy, B., 2003 Distribution of meiotic recombination sites. Trends Genet. **19:** 514–522.

Galagan, J. E., and E. U. Selker, 2004 RIP: the evolutionary cost of genome defense. Trends Genet. **20:** 417–423.

Gale, L. R., L.-F. Chen, C. A. Hernick, K. Takamura and H. C. Kistler, 2002 Population analysis of *Fusarium graminearum* from wheat fields in eastern China. Phytopathology **92:** 1315–1322.

Gerton, J. L., J. deRisi, R. Shroff, M. Lichten, P. O. Brown *et al.*, 2000 Global mapping of meiotic recombination hotspots and coldspots in the yeast *Saccharomyces cerevisiae*. Proc. Natl. Acad. Sci. USA **97:** 11383–11390.

Hou, Z. M., C. Y. Xue, Y. L. Peng, T. Katan, H. C. Kistler *et al.*, 2002 A mitogen-activated protein kinase gene (*MGV1*) in *Fusarium graminearum* is required for female fertility, heterokaryon formation, and plant infection. Mol. Plant-Microbe Interact. **15:** 1119–1127.

Howson, W. T., R. C. McGinnis and W. L. Gordon, 1963 Cytological studies on the perfect stage of some species of *Fusarium*. Can. J. Genet. Cytol. **5:** 60–64.

Johnson, G. D., and G. M. Araujo, 1981 A simple method of reducing the fading of immunofluorescence during microscopy. J. Immunol. Methods **43:** 349–350.

Jurgensen, J. E., R. L. Bowden, K. A. Zeller, J. F. Leslie, N. J. Alexander *et al.*, 2002 A genetic map of *Gibberella zeae* (*Fusarium graminearum*). Genetics **160:** 1451–1460.

Justesen, A. F., C. J. Ridout and M. S. Hovmøller, 2002 The recent history of *Puccinia striiformis* f. sp. *tritici* in Denmark as revealed by disease incidence and AFLP markers. Plant Pathol. **51:** 13–23.

Kistler, H. C., and V. P. W. Miao, 1992 New modes of genetic change in filamentous fungi. Annu. Rev. Phytopathol. **30:** 131–152.

Klittich, C. J. R., and J. F. Leslie, 1988 Nitrate reduction mutants of *Fusarium moniliforme* (*Gibberella fujikuroi*). Genetics **118:** 417–423.

Luikart, G., P. R. England, D. Tallmon, S. Jordan and P. Taberlet, 2003 The power and promise of population genomics: from genotyping to genome typing. Nat. Rev. Genet. **4:** 981–994.

McMullen, M., R. Jones and D. Gallenberg, 1997 Scab of wheat and barley: a re-emerging disease of devastating impact. Plant Dis. **81:** 1340–1348.

Mewes, H. W., C. Amid, R. Arnold, D. Frishman, U. Güldener *et al.*, 2004 MIPS: analysis and annotation of proteins from whole genomes. Nucleic Acids Res. **32:** D41–D44.

Nachman, M. W., 2002 Variation in recombination rate across the genome: evidence and implications. Curr. Opin. Genet. Dev. **12:** 657–663.

Neff, M. M., E. Turk and M. Kalishman, 2002 Web-based primer design for single nucleotide polymorphism analysis. Trends Genet. **18:** 613–615.

O'Donnell, K., H. C. Kistler, B. K. Tacke and H. H. Casper, 2000 Gene genealogies reveal global phylogeographic structure and reproductive isolation among lineages of *Fusarium graminearum*, the fungus causing wheat scab. Proc. Natl. Acad. Sci. USA **97:** 7905–7910.

O'Donnell, K., T. J. Ward, D. M. Geiser, H. C. Kistler and T. Aoki, 2004 Genealogical concordance between the mating type locus and seven other nuclear genes supports formal recognition of nine phylogenetically distinct species within the *Fusarium graminearum* clade. Fungal Genet. Biol. **41:** 600–623.

Rooney, A. P., and T. J. Ward, 2005 Evolution of a large ribosomal RNA multigene family in filamentous fungi: birth and death of a concerted evolution paradigm. Proc. Natl. Acad. Sci. USA **102:** 5084–5089.

Shirane, N., M. Masuko and Y. Hayashi, 1988 Nuclear behavior and division on germinating conidia of *Botrytis cinerea*. Phytopathology **78:** 1627–1630.

Stam, P., 1993 Construction of integrated genetic linkage maps by means of a new computer package; JoinMap. Plant J. **3:** 739–744.

Stumpf, P. H., and G. A. T. McVean, 2003 Estimating recombination rates from population-genetic data. Nat. Rev. Genet. **4:** 959–968.

Suga, H., L. R. Gale and H. C. Kistler, 2004 Development of VNTR markers for two *Fusarium graminearum* clade species. Mol. Ecol. Notes **4:** 468–470.

Taga, M., and M. Murata, 1994 Visualization of mitotic chromosomes in filamentous fungi by fluorescence staining and fluorescence in situ hybridization. Chromosoma **103:** 408–413.

Taga, M., M. Murata and H. Saito, 1998 Comparison of different karyotyping methods in filamentous ascomycetes—a case study of *Nectria haematococca*. Mycol. Res. **102:** 1355–1364.

Taga, M., D. Tsuchiya and M. Murata, 2003 Dynamic changes of rDNA condensation state during mitosis in filamentous fungi revealed by fluorescence in situ hybridization. Mycol. Res. **107:** 1012–1020.

Trail, F., J.-R. Xu, P. San Miguel, R. G. Halgren and H. C. Kistler, 2002 Analysis of expressed sequence tags from *Gibberella zeae* (anamorph *Fusarium graminearum*). Fungal Genet. Biol. **38:** 187–197.

Tsuchiya, D., H. Koga and M. Taga, 2004 Scanning electron microscopy of mitotic nuclei and chromosomes in filamentous fungi. Mycologia **96:** 208–210.

Van Ooijen, J. W., and R. E. Voorrips, 2001 *JoinMap 3.0. Software for the Calculation of Linkage Maps*. Plant Research International, Wageningen, The Netherlands.

Vos, P., R. Hogers, M. Bleeker, M. Reijans, T. Van De Lee *et al.*, 1995 AFLP: a new technique for DNA fingerprinting. Nucleic Acids Res. **23:** 4407–4414.

Ward, T. J., J. P. Bielawski, H. C. Kistler, E. Sullivan and K. O'Donnell, 2002 Ancestral polymorphism and adaptive evolution in the trichothecene mycotoxin gene cluster of phytopathogenic *Fusarium*. Proc. Natl. Acad. Sci. USA **99:** 9278–9283.

Zeller, K. A., R. L. Bowden and J. F. Leslie, 2004 Population differentiation and recombination in wheat scab populations of *Gibberella zeae* from the United States. Mol. Ecol. **13:** 563–571.

Zolan, M. E., 1995 Chromosome-length polymorphism in fungi. Microbiol. Rev. **59:** 686–698.

Communicating editor: M. S. Sachs